

## Supplementary Information for "Nanoscale mechanics by tomographic contact resonance atomic force microscopy"

Gheorghe Stan,<sup>1,2\*</sup> Santiago D. Solares,<sup>2</sup> Bede Pittenger,<sup>3</sup> Natalia Erina,<sup>3</sup> and Chanmin Su<sup>3</sup>

<sup>1</sup>Material Measurement Laboratory, National Institute of Standards and Technology, Gaithersburg, Maryland, 20899, USA

<sup>2</sup>Department of Mechanical Engineering, University of Maryland, College Park, Maryland, 20742, USA

<sup>3</sup>AFM Business Unit, Bruker-Nano Inc., Santa Barbara, California, 93117, USA

### I. DYNAMICALLY INDENTED ELASTOMERS BY A FLAT PUNCH

Depending on the nature of contact and materials probed, the elastic deformation of the tip-sample contact can be adequately described by different contact mechanics models. In some cases when adhesive forces are negligible (*e.g.*, contact on stiff materials), a simple contact mechanics model like Hertz model provides a sufficiently accurate description. However, as is the case for most elastomers, adhesive forces need to be considered as well. It is believed that the two possible extreme cases when adhesive forces manifest themselves in tip-sample contacts are described by two models for elastic deformation: the Derjaguin, Muller and Toporov (DMT) model<sup>34</sup>, which includes long-range adhesive forces outside the contact area (like van der Waals forces), and the Johnson, Kendall and Roberts (JKR) model,<sup>35</sup> which includes short-range adhesive forces acting inside the contact area (like chemical forces). Transitional descriptions between the two limits have been formulated either within analytical models<sup>37,39</sup> or empirical equations.<sup>38</sup> For simplicity we adopted the Schwarz model<sup>39</sup> to derive the necessary equations describing our tip-sample contact mechanics.

In the Schwarz model, the work of adhesion  $\gamma$  is separated into two components,  $\gamma = w_1 + w_2$ , to acknowledge both contributions from short-range adhesive forces and long-range adhesive forces. The short-range adhesive forces contribute as a delta function similar to the JKR model, with  $w_1$  being the integral area under the delta function. On the other hand, the long-range forces are treated similar to the DMT model, with an extra adhesive force of the form  $F_2 = 2\pi R w_2$ , where  $R$  is the tip radius. The proportion between the two contributions, short versus long adhesive forces, comes naturally by introducing a transition parameter  $\tau_1$  defined as the square root of the ratio between  $w_1$  and  $\gamma$ :

$$\tau_1 = \sqrt{\frac{w_1}{\gamma}} = \sqrt{\frac{w_1}{w_1 + w_2}}. \quad (1)$$

In this formulation, the DMT limit is obtained when  $\tau_1 = 0$  ( $w_1 = 0$ ) and the JKR limit is obtained when  $\tau_1 = 1$  ( $w_2 = 0$ ). The adhesive force is defined as a superposition of JKR and DMT contributions,  $F_a = -\frac{3}{2}\pi R w_1 - 2\pi R w_2$ , and is added to the effective applied force  $F$ . With that, a Hertz-type tip-sample interaction,  $a = (3RF/4E^*)^{1/3}$ , provides the force dependences for the contact radius and indentation depth as:

$$a = \left(\frac{3R}{4E^*}\right)^{1/3} \left(\frac{\tau_1}{\sqrt{4 - \tau_1^2}} \sqrt{3F_a} + \sqrt{F + F_a}\right)^{2/3} \quad (2)$$

and

$$\delta = \frac{a^2}{R} - \frac{\tau_1}{\sqrt{4 - \tau_1^2}} \sqrt{\frac{4aF_a}{RE^*}}, \quad (3)$$

respectively. Here,  $E^* = ((1 - \nu_T^2)/E_T + (1 - \nu_S^2)/E_S)^{-1}$  is defined as the reduced elastic modulus between tip and sample, with  $\nu_T$ ,  $E_T$  and  $\nu_S$ ,  $E_S$  being the Poisson's ratio and Young's modulus for the tip and sample, respectively. In the case of compliant materials,  $E^*$  is comparable with the indentation modulus of the indented sample  $M_S =$

---

\* Electronic mail: gheorghe.stan@nist.gov

$(1 - \nu_S^2)/E_S$  as the contribution from the much stiffer tip,  $1/M_T$ , is negligible. The DMT and JKR expressions for  $a$  and  $\delta$  are readily obtained from (2) and (3) by particularizing  $\tau_1$  for each of the two cases.

The contact stiffness is defined in general as the derivative of the applied force with respect to deformation,  $k_c^* = \partial F / \partial \delta$ . By introducing  $a$  and  $\delta$  from (2) and (3) into  $k_c^{*-1} = \partial \delta / \partial F = (\partial \delta / \partial a)(\partial a / \partial F)$ , the contact stiffness is obtained as

$$k_c^* = (6RE^{*2})^{1/3} \frac{\sqrt{3(4 - \tau_1^2)}\sqrt{F + F_a} \left( \frac{\tau_1}{\sqrt{4 - \tau_1^2}}\sqrt{3F_a} + \sqrt{F + F_a} \right)^{2/3}}{2\tau_1\sqrt{F_a} + \sqrt{3(4 - \tau_1^2)}\sqrt{F + F_a}}. \quad (4)$$

The expressions for DMT and JKR contact stiffness for a spherical tip indenting a flat substrate can be obtained from (4) by replacing  $\tau_1$  by either 0 or 1.<sup>28,36</sup>

The above description for the contact stiffness works well in the case of a spherical tip quasi-statically (low cycling frequency) indenting a flat surface. However, a particular case was rationalized for the dynamic (high cycling frequency) indentation of an elastomer. Thus, in the case of a fast oscillation, it has been shown<sup>40,41</sup> that viscoelastic effects can hinder the peripheral variations imposed by the oscillation onto the contact area. As a result, the contact area remains approximately constant during an oscillation and the contact geometry resembles that of a "flat punch" configuration. Therefore, in the limit of the dynamic flat punch approximation, the stiffness response of a dynamically indented polymer is equivalent to that of a flat punch with the contact radius of the static configuration (Schwarz model in our case). With (2), the expression for the contact stiffness of a dynamic flat punch in the Schwarz model becomes

$$k^* = 2aE^* = (6RE^{*2})^{1/3} \left( \frac{\tau_1}{\sqrt{4 - \tau_1^2}}\sqrt{3F_a} + \sqrt{F + F_a} \right)^{2/3}. \quad (5)$$

Also, by introducing  $a = k^*/2E^*$  into (3), the deformation  $\delta$  can be expressed in terms of the contact stiffness of a dynamic flat punch:

$$\delta = \frac{k^{*2}}{4RE^{*2}} - \frac{\tau_1}{\sqrt{4 - \tau_1^2}}\sqrt{\frac{2k^*F_a}{RE^{*2}}}. \quad (6)$$

This can be rewritten as:

$$\delta/\sqrt{k^*} = \alpha + \beta k^{*3/2}, \quad (7)$$

with  $\alpha = -\frac{\tau_1}{\sqrt{4 - \tau_1^2}}\sqrt{2F_a/(RE^{*2})}$  being the  $y$ -intercept and  $\beta = 1/(4RE^{*2})$  the slope of the linear dependence of  $\delta/\sqrt{k^*}$  vs  $k^{*3/2}$ . As shown in Fig. S1, when plotted in  $\delta/\sqrt{k^*}$  vs  $k^{*3/2}$  coordinates, the two contact geometries, spherical tip and flat punch on a flat surface, are differentiated from each other through  $\tau_1$ . It follows from here that the elastic reduced modulus can be calculated solely from the slope,

$$E^* = 1/\sqrt{4R\beta} \quad (8)$$

and the transition parameter  $\tau_1$  from the slope and  $y$ -intercept values,

$$\tau_1 = \frac{2|\alpha|}{\sqrt{8F_a\beta + \alpha^2}}. \quad (9)$$

Within the dynamic flat punch limit, a calibration for  $\delta$  can be easily carried out by calculating the indentation depth at the maximum negative applied force,  $F = -F_a$ , as a function of two measured values of contact stiffness:  $k_a^*$ - the contact stiffness at  $F = -F_a$  and  $k_0^*$ - the contact stiffness at  $F = 0$ . From the above equations:

$$k_a^* = \left( 18RE^{*2}F_a \frac{\tau_1^2}{4 - \tau_1^2} \right)^{1/3} \quad (10)$$

and

$$k_0^* = (6RE^{*2}F_a)^{1/3} \left( 1 + \frac{\tau_1\sqrt{3}}{\sqrt{4 - \tau_1^2}} \right)^{2/3}. \quad (11)$$

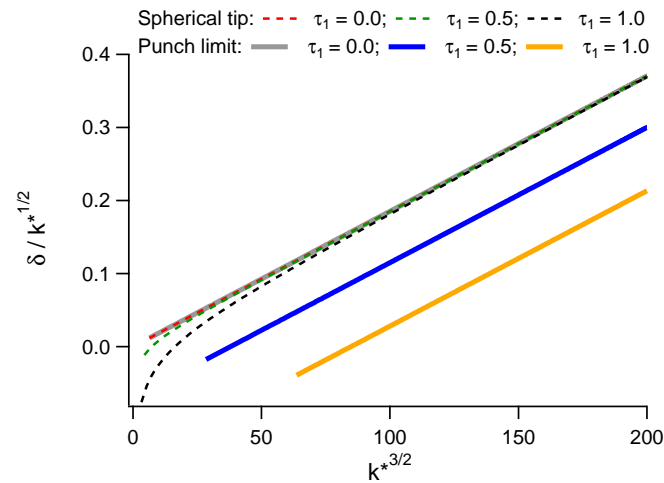


FIG. S1: In the Schwarz model, the distinction between contact geometries with a spherical tip and a "dynamic flat punch" indenting a flat surface is evident when  $\delta/\sqrt{k^*}$  is plotted versus  $k^{*3/2}$  for various values of  $\tau_1$ .

By taking the ratio of these two quantities, we can define the parameter

$$\kappa = \left(\frac{k_a^*}{k_0^*}\right)^3 = \frac{3\tau_1^2}{\left(\sqrt{4 - \tau_1^2} + \tau_1\sqrt{2}\right)^2}. \quad (12)$$

By inverting (12), the transition parameter  $\tau_1$  can be found as a function of  $\kappa$

$$\tau_1 = 2/\sqrt{1 + 3\left(\sqrt{1/\kappa} - 1\right)^2}. \quad (13)$$

and used in (10) and (6) to calculate the indentation depth at  $F = -F_a$ :

$$\delta_a = -\frac{F_a}{2k_a^*} \left[ \left(\frac{k_0^*}{k_a^*}\right)^{3/2} - 1 \right]^{-2}. \quad (14)$$

$\delta_a$  given by (14) can be used as a reference measurement to calibrate the indentation depths when  $F_a$ ,  $k_a^*$  and  $k_0^*$  are known. This calibration procedure for the indentation depth was applied for the analysis of stiffness-depth curves.

As it can be seen in Fig. S1, the two geometries are indistinguishable for  $\tau_1 = 0$ . However, for non-zero values of  $\tau_1$ , the plots for the two geometries can be easily distinguished. On one hand, the dependence is slightly non-linear and there is not a significant change in the case of a spherical tip as  $\tau_1$  ranges from 0 to 1. On the other hand, in the dynamic flat punch limit, the dependence is linear for any value of  $\tau_1$  and large shifts are observed with changes in  $\tau_1$  while the slope is preserved over the entire range. The calculations here were performed for an applied force ranging from  $-5$  nN to  $100$  nN,  $F_a = 5$  nN,  $R = 15$  nm, and  $E^* = 3$  GPa. In our experiment, the stiffness-depth curves measured on both PP and PS resemble the theoretical dependences of a dynamic flat punch on flat surface.

- 
- [1] N. A. Burnham and R. J. Colton, *J. Vac. Sci. Technol. A*, 1989, **7**, 2906.  
 [2] P. Maiwald, H. J. Butt, S. A. C. Gould, C. B. Prater, B. Drake, J. A. Gurley, V. B. Elings and P. K. Hansma, *Nanotechnology*, 1991, **2**, 103.  
 [3] S. Magonov, V. B. Elings and M. Whangbo, *Surface Sci.*, 1997, **375**, L385.  
 [4] O. Sahin, S. Magonov, C. Su, C. F. Quate and O. Solgaard, *Nature Nanotech.*, 2007, **2**, 507.  
 [5] S. Jesse, S. V. Kalinin, R. Proksch, A. P. Baddorf and B. J. Rodriguez, *Nanotechnology*, 2007, **18**, 435503.  
 [6] B. Pittenger, N. Erina and C. Su, *Bruker Application Note AN128*, 2010.  
 [7] R. Garcia and E. T. Herruzo, *Nature Nanotech.*, 2012, **7**, 217.

- [8] U. Rabe, S. Amelio, M. Kopycinska, S. Hirsekorn, M. Kempf, M. Göken and W. Arnold, *Surf. Interface Anal.*, 2002, **33**, 65.
- [9] H. Wagner, D. Bedorf, S. Küchemann, M. Schwabe, B. Zhang, W. Arnold and K. Samwer, *Nature Materials*, 2011, **10**, 439.
- [10] G. Stan, S. W. King and R. F. Cook, *Nanotechnology*, 2012, **23**, 215703.
- [11] B. Gotsmann, C. Seidel, B. Anczykowski and H. Fuchs, *Phys. Rev. B*, 1999, **60**, 11051.
- [12] P. A. Yuya, D. C. Hurley and J. A. Turner, *J. Appl. Phys.*, 2008, **104**, 074916.
- [13] R. Garcia, C. J. Gomez, N. F. Martinez, S. Patil, C. Dietz and R. Magerle, *Phys. Rev. Lett.*, 2006, **97**, 016103.
- [14] G. Chawla and S. D. Solares, *Appl. Phys. Lett.*, 2011, **99**, 074103.
- [15] A. Raman, S. Trigueros, A. Cartagena, A. P. Z. Stevenson, M. Susilo, E. Nauman and S. Antoranz Contera, *Nature Nanotech.*, 2011, **6**, 809.
- [16] N. Gavara and R. S. Chadwick, *Nature Nanotech.*, 2012, **7**, 733.
- [17] H. Hölscher, S. M. Langkat, A. Schwarz and R. Wiesendanger, *Appl. Phys. Lett.*, 2002, **81**, 4428.
- [18] L. Gross, F. Mohn, N. Moll, P. Liljeroth and G. Meyer, *Science*, 2009, **325**, 1110.
- [19] B. J. Albers, T. C. Schwendemann, M. C. Baykara, N. Pilet, M. Liebmann, E. I. Altman and U. D. Schwarz, *Nature Nanotech.*, 2009, **4**, 307.
- [20] T. Fukuma, Y. Ueda, S. Yoshioka and H. Asakawa, *Phys. Rev. Lett.*, 2010, **104**, 016101.
- [21] S. Fremy, S. Kawai, R. Pawlak, T. Glatzel, A. Baratoff and E. Meyer, *Nanotechnology*, 2012, **23**, 055401.
- [22] E. T. Herruzo, H. Asakawa, T. Fukuma and R. Garcia, *Nanoscale*, 2013, **5**, 2678.
- [23] J. E. Schmutz, H. Hölscher, D. Ebeling, M. M. Schäfer and B. Anczykowski, *Ultramicroscopy*, 2007, **107**, 875.
- [24] E.-C. Spitzner, C. Riesch and R. Magerle, *ACS Nano*, 2011, **5**, 315.
- [25] L. Tetard, A. Passian and T. Thundat, *Nature Nanotech.*, 2010, **5**, 105.
- [26] M. Stolz, R. Gottardi, R. Raiteri, S. Miot, I. Martin, R. Imer, U. Staufer, A. Raducanu, M. Düggelin, W. Baschong, A. U. Daniels, N. F. Friederich, A. Aszodi and U. Aebi, *Nature Nanotech.*, 2009, **4**, 186.
- [27] A. Fuhrmann, J. R. Staunton, V. Nandakumar, N. Banyai, P. C. W. Davies and R. Ros, *Phys. Biol.*, 2011, **8**, 015007.
- [28] G. Stan, S. W. King and R. F. Cook, *J. Mater. Sci.*, 2009, **24**, 2960.
- [29] U. Rabe, K. Janser and W. Arnold, *Rev. Sci. Instrum.*, 1996, **67**, 3281.
- [30] K. Yamanaka and S. Nakano, *Japan. J. Appl. Phys.*, 1996, **35**, 3787.
- [31] L. Nony and A. Baratoff, *Phys. Rev. B*, 2006, **74**, 235439.
- [32] H. Hölscher, B. Gotsmann and A. Schirmeisen, *Phys. Rev. B*, 2003, **68**, 153401.
- [33] J. P. Killgore, D. G. Yablon, A. H. Tsou, A. Gannepalli, P. A. Yuya, J. A. Turner, R. Proksch and D. C. Hurley, *Langmuir*, 2011, **27**, 13983.
- [34] B. V. Derjaguin, V. M. Müller and Y. P. Toporov, *J. Colloid Interface Sci.*, 1975, **53**, 314.
- [35] K. L. Johnson, K. Kendall and A. D. Roberts, *Proc. R. Soc. London A*, 1971, **324**, 301.
- [36] O. Piétrement and M. Tryoyon, *J. Colloid Interface Sci.*, 2000, **226**, 166.
- [37] D. Maugis, *J. Colloid Interface Sci.*, 1992, **150**, 243.
- [38] R. W. Carpick, D. F. Ogletree and M. Salmeron, *J. Colloid Interface Sci.*, 1999, **211**, 395.
- [39] U. D. Schwarz, *J. Colloid Interface Sci.*, 2003, **261**, 99.
- [40] K. J. Wahl, A. S. Asif, J. A. Greenwood and K. L. Johnson, *J. Colloid Interface Sci.*, 2006, **296**, 178.
- [41] J. A. Greenwood and K. L. Johnson, *J. Colloid Interface Sci.*, 2006, **296**, 284.
- [42] A. Matsuoaka and B. Maxwell, *J. Polymer Sci.*, 1958, **32**, 131.